# Improved mathematical model for a falling film sulfonation reactor

**ARTICLE** *in* INDUSTRIAL & ENGINEERING CHEMISTRY RESEARCH · SEPTEMBER 1988

Impact Factor: 2.59 · DOI: 10.1021/ie00081a023



**3 AUTHORS**, INCLUDING:

Claudi Mans
University of Barcelona
**34** PUBLICATIONS **105** CITATIONS
SEE PROFILE

Josep Costa
University of Barcelona
**33** PUBLICATIONS **510** CITATIONS
SEE PROFILE

GENERAL RESEARCH

# Improved Mathematical Model for a Falling Film Sulfonation Reactor

**J. Gutiérrez-González,* C. Mans-Teixidó, and J. Costa-López**
*Department of Chemical Engineering, Faculty of Chemistry, University of Barcelona, Martí i Franquès 1, 08028 Barcelona, Spain*

A mathematical model of a process in which an exothermic, second-order reaction takes place in a falling film reactor was developed. This model is applicable to a process in which any step, liquid mass transfer, reaction rate, or gas mass transfer, can affect the process rate. The model includes a turbulent diffusivity term for the liquid mass transfer, valid through the entire liquid film. The mathematical model predicts conversions and interfacial temperatures as the most important variables for product yields and product quality. Its validity was proved by means of experimental sulfonation of dodecylbenzene. This model could be applicable to any process that takes place in a falling film reactor.

The sulfonation or sulfation reaction is generally utilized for the production of detergents. By means of this reaction, hydrophilic groups—$CSO_3^-$ or $COSO_3^-$—are introduced in organic compounds with hydrophobic chains. The sulfonation agent $SO_3$ is one of the most utilized because it has some advantages with regard to other agents: sulfuric acid or oleum. Two of these advantages are that it reacts stoichiometrically and without secondary products. However, $SO_3$ reaction with organic compounds is very exothermic, $-1.68 \times 10^6$ J/mol of $SO_3$, for the sulfonation of dodecylbenzene and requires good refrigeration to avoid the degradation of the products.

A frequently utilized apparatus for the sulfonation or sulfation of organic compounds is the falling film reactor. Other types of reactors are the stirred tank, the Votator, and the spray reactor.

In the falling film reactor, a liquid film of the organic reactant falls by gravity, completely wetting the solid wall and contacting the $SO_3$ vapor which is diluted in an inert gas, generally air. The solid surface is refrigerated by externally circulating water. Due to the high surface to volume ratio of liquid in the column, efficient heat elimination takes place.

In the process of sulfonation/sulfation, the liquid normally circulates in a laminar flow, and the gas, cocurrently with the liquid, circulates in a turbulent flow.

The simple geometry of the system and the laminar circulation of the liquid enables us to describe the fluid dynamics, the mass transfer, and the heat transfer through equations that can be analytically or numerically integrated.

Different models are proposed in the bibliography.

0888-5885/88/2627-1701$01.50/0 

Johnson and Crynes (1974) assumed that the reaction takes place only at the gas–liquid interface. They made use of the Gilliland–Sherwood empirical equation (1934) to calculate the mass-transfer coefficient for the transfer between the gas and the interface. The coefficient for the heat transfer between the gas and the interface was calculated by means of a modified standard Nusselt-type equation, and the coefficient for the heat transfer to the solid wall was estimated by means of the Davis and David correlation (1964). Taking into account these coefficients, and assuming a linear temperature profile in the liquid film, Johnson and Crynes (1974) obtained the temperatures of the process.

Davis et al. (1979) propounded another model where they completely described the fluid dynamics of the liquid film determining the film thickness and the velocity profiles. Like Johnson and Crynes (1974), they also assumed that the reaction takes place only at the interface, and they also applied the Gilliland–Sherwood equation to determine the $SO_3$-transfer coefficient. Davis et al. (1979) determined through the laminar microscopic balance equation the heat transfer in the liquid film and from this the temperatures of the process. They numerically solved this equation, in integrated form, to get a stable solution.

In both models, the reaction takes place at the interface. This implies that the process rate is controlled by the $SO_3$ transfer to the interface. It also means that the reaction is instantaneous and that the liquid reactant transfer rate is much greater than the $SO_3$ gas-transfer rate. These hypotheses can be valid at the beginning of the reactor, but due to the high viscosity of the sulfonated or sulfated products and the high conversions obtained in the process, the transfer of the liquid reactant will be slower in other zones of the reactor, where conversions are greater. If the liquid reactant transfer rate were not much greater than the gas reactant transfer rate, the liquid transfer would affect the process rate, as Davis et al. have admitted. However, their model does not take into account this effect. Moreover, the presence of an unsulfonated product and free $H_2SO_4$ in the sulfonation product cannot be explained by models assuming that the reaction is taking place only at the interface.

The purpose of this paper is to develop an improved mathematical model for the falling film reactor. In contrast to the previously mentioned model, we do not assume in our model that any step—liquid transfer, gas transfer, or reaction rate—can alone control the process rate, but the three together can affect it.

Our mathematical model will predict the influence of the geometric variables, diameter and length of the reactor, and the process variables, $SO_3$/liquid reactant mole ratio, $SO_3$ mole fraction in the gas, and refrigeration water temperature, on the conversion and temperatures of the sulfonated product. The temperatures reached in the process are extremely important since high temperature results in a colored product.

The partial difference equations which describe mass and heat transfer in the liquid are solved by finite difference methods, using implicit expressions in order to get a stability in the solution.

The validity of the mathematical model proposed is established by comparing its predictions with experimental results for the sulfonation of dodecylbenzene. These experiments were carried out with different values for the variables of reactor length, $SO_3$/dodecylbenzene mole ratio, and $SO_3$ mole fraction in the gas.

## Qualitative Description of the Model

In Figure 1, a scheme of the liquid film is shown. The

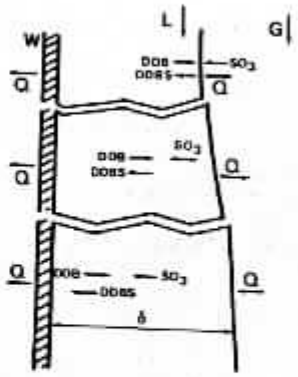


**Figure 1.** Qualitative descriptions of the phenomena occurri a falling film sulfonation reactor.

different phenomena taking place are indicated.

At the beginning of the reactor, diluted $SO_3$ contac film of pure liquid reactant. The proocess rate is limited by the $SO_3$ transfer from the bulk gas to the terface and by the reaction rate. The film temperat is low, so the $SO_3$ solubility is high. The process rat high, and a large amount of heat is generated and transferred to the cooling water and to the gas.

In those zones where conversion increases, the resista to mass transfer in the liquid film begins to be signific and it brings about the increase of the film thickness ( creased viscosity) and the decrease of diffusion. T $SO_3$-transfer rate in the gas decreases because the c centration in this phase diminishes. The reaction prod diffuses toward the reactor wall.

In the zones near the end of reactor, where conversi is high, the reaction rate is low because of the decrease reactant concentration and the low temperatures. Th the process rate is controlled mainly by the mass trans in the liquid, but the reaction rate also affects it.

The mathematical model will consist of microscop balance equations in the liquid phase with their cor sponding boundary conditions. Through these equatio velocity, concentration, and temperature profiles are o tained. The equations are for steady-state operatio common in industrial and laboratory reactors.

The principal assumptions are as follows:

The liquid circulates in a laminar flow, and the g circulates cocurrently in a turbulent flow.

The liquid film is symmetric with respect to the react axis.

$SO_3$ solubility in the liquid reactant and in the reactio products is ideal according to Henry's law.

The only reaction that takes place is the mono sulfonation of dodecylbenzene (DDB) to obtain dodecy benzenesulfonic acid (DDBS).

The film thickness is small compared to the colum radius.

"A priori", there are no controlling steps for mas transfer.

Liquid reactant DDB and product DDBS are assume to be nonvolatile at working temperatures.

The mathematical model equations are indicated i Table I. These equations are explained below according to the momentum, mass, or heat transfer taking place

## Momentum Transfer

For this system, eddy viscosity, $\nu_E$, can be disregarded with respect to kinematic viscosity, and $\nu_E$ does not appear in the Navier–Stokes equations, which, when applied to steady-state flow and when taking into account the in-

**Table I. Equations of the Mathematical Model**

$$v_z = \frac{g}{\nu}\left(\delta y - \frac{y^2}{2}\right) - \frac{\tau_G y}{\mu} \quad (1)$$

$$\tau_G = \frac{\rho g}{3\mu}\delta^3 - \frac{\tau_G \delta^2}{2\mu} \quad (2)$$

$$\tau_G = f\rho_G U^2 \quad (3)$$

$$f = 0.04ARe^{1/4} \quad \text{where } A = A_0 - A_1 z \quad (4)$$

$$k_G/u_* = BSc^{-0.6704} \quad (5)$$

$$u_* = (\tau_G/\rho_G)^{1/2} \quad (6)$$

$$N_{SO_3}{}^G = k_G(C_{SO_3}{}^G - mC_{SO_3}{}^L) \quad (7)$$

$$v_z \frac{\partial C_{DDB}}{\partial z} = \frac{\partial}{\partial y}\left[(D_{DDB} + D_E)\frac{\partial C_{DDB}}{\partial y}\right] - kC_{DDB}C_{SO_3} \quad (8)$$

$$v_z \frac{\partial C_{SO_3}}{\partial z} = \frac{\partial}{\partial y}\left[(D_{SO_3} + D_E)\frac{\partial C_{SO_3}}{\partial y}\right] - kC_{DDB}C_{SO_3} \quad (9)$$

$$\frac{\nu_E}{\nu} = -0.5 + 0.5\left[1 + 0.64(y^+)^2\frac{\tau}{\tau_w} \times \left[1 - \exp\left[\frac{-y^+(\tau/\tau_w)^{1/2}}{A^+}\right]\right]\right]^{1/2} \quad (10)$$

$$\frac{\tau}{\tau_w} = 1 - \left[\frac{\tau_L}{\tau_G + \tau_L}\right]^3 (y^+/\delta^+) \quad (11)$$

$$Sc_E = \frac{\nu_E}{D_E} = \frac{1 - \exp(-y^+(\tau/\tau_w)^{1/2}/A^+)}{1 - \exp(-y^+(\tau/\tau_w)^{1/2}/B^+)} \quad (12)$$

$$B^+ = Sc^{-1/2}\sum_{i=1}^{5} C_i(\log Sc)^{(i-1)} \quad (13)$$

$$v_z \frac{\partial(\rho C_p T)}{\partial z} = -\frac{\partial}{\partial y}\left(-K_L\frac{\partial T}{\partial y}\right) + (\Delta H)_R{}^* kC_{DDB}C_{SO_3} \quad (14)$$

$$\frac{1}{U_L} = \frac{1}{\frac{K_w d_{lm}}{d_{ex}}} + \frac{1}{h_R\frac{d_{ex}}{d_{in}}} \quad (15)$$

$$h_G/u_* = BPr^{-0.704} \quad (16)$$

teraction between gas and liquid, describe the laminar flow of the liquid film.

In order to obtain the velocity profiles through eq 1, the shear stress at the gas–liquid interface, $\tau_G$, has to be determined. This value is related to the friction factor, $f$, by eq 3. The value of $f$ can be determined by means of equations such as that of Blasius, eq 4. In eq 4, a correction term, $A$, has been introduced to account for the gas entrance effects. In the model, it is assumed that $A$ decreases linearly with the distance from the reactor entrance.

The film thickness, $\delta$, is calculated through eq 2 by iteration. Entrance effects for the liquid film are not considered because, according to the Pierson and Whitaker equation (1977), the entrance length is negligible (<1 mm). Neither are outlet effects considered because we do not have the conditions in which these effects would take place, according to Cook and Reginald (1973).

## Mass Transfer

For the gas in turbulent flow, mass-transfer coefficients are calculated by means of an empirical equation. Johnson and Crynes (1974) and Davis et al. (1979) used the well-known Gilliland–Sherwood equation, introducing a factor of 2 to account for interfacial ripple enhancement of the mass transfer, although this equation had been determined to be used for systems with ripples. In this work, it was considered more appropriate to use McReady and Hanratty's equation (1984), eq 5, with a correction term, $B$, determined later by correlation with experimental results. In eq 5, $u_*$, the characteristic turbulence velocity, is calculate from $\tau_G$ (eq 6). At the interface, it is assumed that Henry's and Raoult's laws are applicable (Mann and Moyes, 1977) to determine the $SO_3$ solubility. The Henry's constant, $m$, is determined from the $SO_3$ vapor pressure. Mass transfer in the gas phase is introduced as a boundary condition in the microscopic balance for the liquid phase.

For the model, only three components are considered in the liquid phase: DDB, DDBS, and $SO_3$. Therefore, two microscopic balances are sufficient to determine the concentration profiles. The microscopic balances of DDB and $SO_3$, for this system, are the eq 8 and 9. In these equations, it is assumed that the reaction is second order (Mann et al., 1982).

Although the liquid flow is laminar, due to the high Schmidt number, eddy mass transfer can be significant, and eddy diffusion, $D_E$, cannot be disregarded with respect to molecular diffusion. So, an eddy diffusion term, $D_E$, as a function of the radial coordinate, $y$, was introduced in the microscopic mass balances.

There are different theoretical and empirical models available for the estimation of $D_E$ (Levich, 1962; Davies, 1972; Henstock and Hanratty, 1979; Jepsen et al., 1966). In this work, a model, originally used to estimate eddy thermal diffusion, $\alpha_E$, propounded by Yih and Liu (1983), was used. The reason for choosing this model was that it takes into account turbulence damping by the solid–liquid and the gas–liquid interfaces, as well as the influence of the interfacial shear stress on the transfer in the liquid. Because of the analogy between mass, heat, and momentum transfers, it is possible to calculate $\alpha_E$ or $D_E$ from $\nu_E$ (Bird et al., 1960). In this work, the same equations used by Yih and Liu to calculate $\alpha_E$ are used to calculate $D_E$ (eq 10–13). Equation 10, with $\tau/\tau_w$ determined through eq 11, permits us to calculate $\nu_E$. $D_E$ is obtained from eq 12 with the value previously calculated for $\nu_E$, and $B^+$ is obtained from eq 13. The coefficient values of these equations are $A^+ = 25.1$, $C_1 = 34.96$, $C_2 = 28.97$, $C_3 = 13.95$, $C_4 = 6.33$, and $C_5 = -1.186$.

## Heat Transfer

Heat transfer in the liquid phase is determined by means of the microscopic heat balance (eq 14). Eddy thermal diffusion is much smaller than thermal diffusion, so it is not introduced in the microscopic balance.

The heat-transfer coefficient in the gas phase, $h_G$, is obtained through eq 16, which is similar to eq 4 used for mass transfer in the gas phase. The overall heat-transfer coefficient for the refrigeration of water is determined through eq 15.

Heat transfer to the refrigerated water and to the gas phase are introduced as boundary conditions in the microscopic heat balance for the liquid phase.

## Boundary Conditions

The initial and boundary conditions required to integrate eq 8, 9, and 14 are shown in Table II. (a) and (d) are the initial conditions. The conditions (b) indicate that the compounds, mathematically and in fact, cannot pass through the wall. The conditions (c) indicate that $SO_3$ crosses the interface at a rate depending on the $SO_3$ gas mass transfer, and that DDB is not volatile and it cannot cross the interface. Condition (e) relates the temperatures of the liquid film to the temperatures of the refrigeration

**Table II. Boundary Conditions**

Mass Transfer

(a) for $z = 0$, $C_{DDB} = C_{DDB}^{0}$, $C_{SO_3} = 0$
(b) for $y = 0$, $\partial C_{DDB}/\partial y = 0$, $\partial C_{SO_3}/\partial y = 0$
(c) for $y = \delta$, $\partial C_{DDB}/\partial y = 0$, $\partial C_{SO_3}/\partial y = (k_G/D_{SO_3})(C_{SO_3}^{G} - mC_{SO_3}^{il})$

Heat Transfer

(d) for $z = 0$, $T = T^0$
(e) for $y = 0$, $K_L\, \partial T/\partial y = U_L(T_{y=0} - T_R)$
(f) for $y = \delta$, $-K_L\, \partial T/\partial y = h_G(T_{y=\delta} - T_G)$

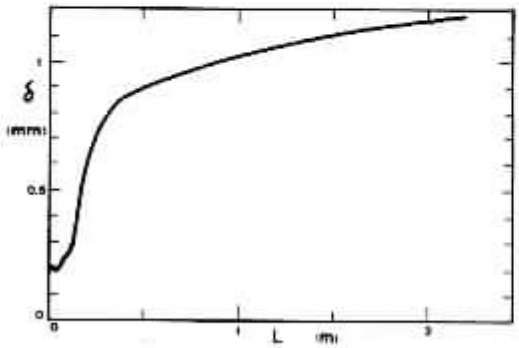


**Figure 2.** Example of longitudinal profile of film thickness.

water. Condition (f) is the heat transfer from the liquid to the gas.

## Physicochemical Properties

The properties of the compounds are obtained from experimental correlations or estimations as follows:

Viscosity and density of DDB and DDBS mixtures are determined from correlations given by Brönstrom (1975).

Thermal conductivities in liquid and gas phases and specific heat capacities are obtained from the data given by Davis et al. (1979).

DDB and DDBS diffusivities are estimated from the Wilke–Chang equations, and diffusivities in the mixture are estimated through the Vignes equation (Reid et al., 1977).

For the reaction heat, the data given by Brönstrom (1975) were used.

Reaction rate was calculated from the data for the kinetic parameters given by Mann et al. (1982).

## Solution of the Mathematical Model

The equation system described above cannot be solved analytically, so this was done numerically.

Concentration profiles are obtained by means of the implicit finite difference method of Laasonen (Lapidus, 1962). This method implies the resolution of $N$ equations ($N$ being the number of annular segments) for the DDB and another system with the same number of equations for the $SO_3$. The systems are solved by matrix calculus. Both systems have the DDB and the $SO_3$ concentrations in common in the reaction term, so the resolution has to be done iteratively.

Velocities at the middle point of each annular segment and eddy diffusivities between every two contiguous segments were determined previously.

The temperature profiles were obtained by the same method. The concentration and temperature profiles permit the calculation of conversion and the new concentration of $SO_3$ in the gas. From these, physical properties, film thickness, velocity profile, and the eddy diffusivity profile that must be applied to the next longitudinal segment are calculated.

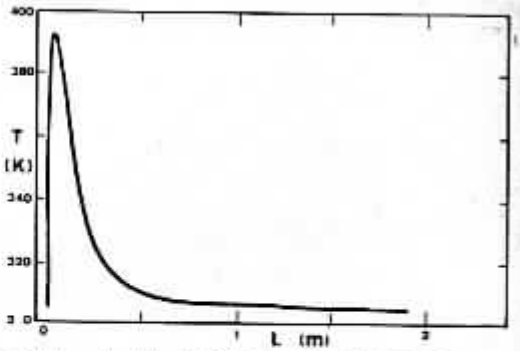


**Figure 3.** Example of longitudinal profile of interfacial temperatu

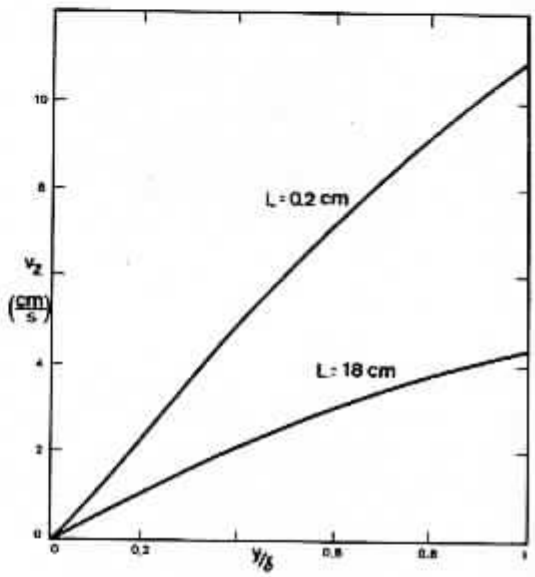


**Figure 4.** Some radial profiles of axial liquid velocity.

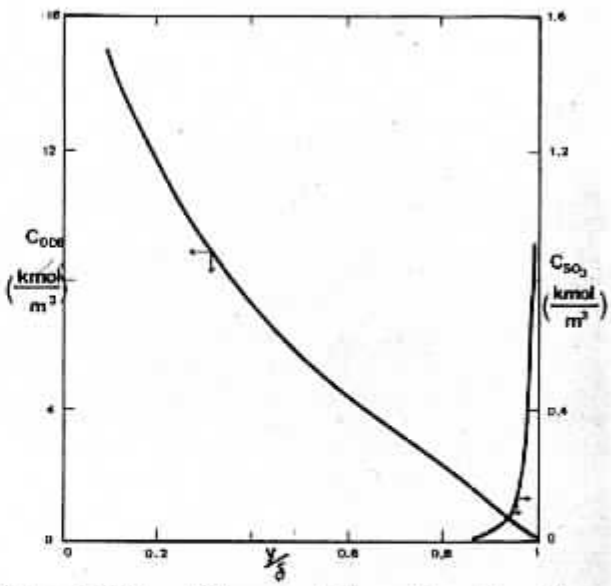


**Figure 5.** DDB and $SO_3$ concentration radial profiles at the entrance zone of the reactor. $SO_3$/DDB mole ratio: 1.10. $SO_3$ mole fraction in the gas: 0.08.

This method of calculation allows the determination of concentrations and temperatures for the entire length of the reactor.

The mathematical model described permits one to calculate the radial profiles of concentration, temperature, and velocity for any column height, as well as longitudinal profiles of conversion and temperatures. In Figures 2 and

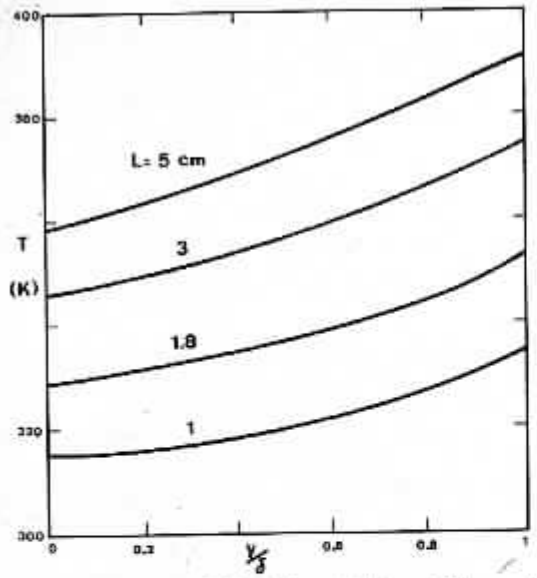


**Figure 6.** Temperature radial profiles at different distances from the top of the reactor.

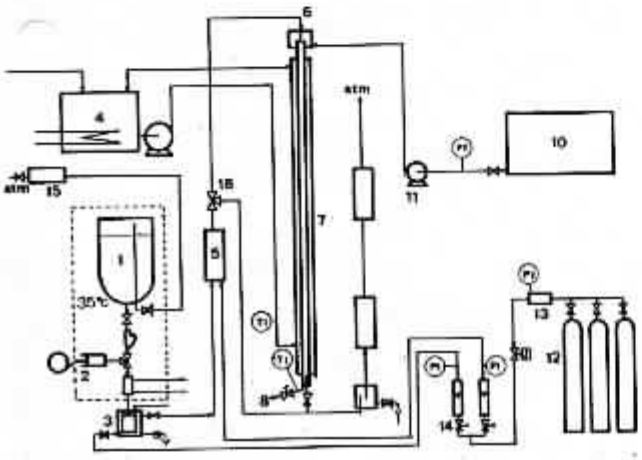


**Figure 7.** Experimental apparatus.

3, examples of longitudinal profiles of film thickness and interfacial temperatures are shown, and in Figures 4–6, examples of radial profiles of temperature, concentration, and velocity can be seen.

A comparison between model predictions and experimental results for conversion will be shown later.

## Experimental Apparatus

In Figure 7, a scheme of the experimental apparatus utilized is shown.

The monotubular falling film reactor (7) is the basic part of this apparatus. The entrances of liquid and gas reactants are at the reactor top, and the outlets of the sulfonated product and the residual gas are at the bottom. Three reactors of stainless steel AISI 316, nominal diameter $^1/_2$ in. (ANSI B36.19), actual interior diameter 1.39 cm, with a wall 3.88 mm thick, and a refrigeration jacket, were utilized. The lengths of the reactors were 0.400, 0.973, and 2.000 m.

The $SO_3$ was stored as a liquid (1) at 35 °C. It was fed by a syringe pump (2) and vaporized by steam heating in a vaporizer (3). The $SO_3$ vapor was diluted to the desired concentration with nitrogen before entering the reactor.

The dodecylbenzene was fed by a gear pump (11). Refrigerated water temperature was controlled in a tank (4) with electric heating and water cooling.

**Table III. Experimental Results**

| expt | reactor length, m | $SO_3$/DDB mole ratio | $SO_3$ mole fraction in gas | mean active matter, % |
|---|---|---|---|---|
| 1 | 0.400 | 1.00 | 0.04 | 74.9 |
| 2 | 0.400 | 1.00 | 0.06 | 76.0 |
| 3 | 0.400 | 1.00 | 0.08 | 74.2 |
| 4 | 0.400 | 1.00 | 0.10 | 70.2 |
| 5 | 0.400 | 1.00 | 0.12 | 73.6 |
| 6 | 0.400 | 1.10 | 0.04 | 83.7 |
| 7 | 0.400 | 1.10 | 0.06 | 81.0 |
| 8 | 0.400 | 1.10 | 0.08 | 80.2 |
| 9 | 0.400 | 1.10 | 0.10 | 80.5 |
| 10 | 0.400 | 1.10 | 0.12 | 75.8 |
| 11 | 0.973 | 1.00 | 0.04 | 87.3 |
| 12 | 0.973 | 1.00 | 0.06 | 83.9 |
| 13 | 0.973 | 1.00 | 0.08 | 83.2 |
| 14 | 0.973 | 1.00 | 0.10 | 79.8 |
| 15 | 0.973 | 1.00 | 0.12 | 76.4 |
| 16 | 0.973 | 1.05 | 0.04 | 89.7 |
| 17 | 0.973 | 1.05 | 0.06 | 87.6 |
| 18 | 0.973 | 1.05 | 0.08 | 85.1 |
| 19 | 0.973 | 1.05 | 0.10 | 80.5 |
| 20 | 0.973 | 1.05 | 0.12 | 83.5 |
| 21 | 0.973 | 1.10 | 0.04 | 90.3 |
| 22 | 0.973 | 1.10 | 0.06 | 87.9 |
| 23 | 0.973 | 1.10 | 0.08 | 85.9 |
| 24 | 0.973 | 1.10 | 0.10 | 86.2 |
| 25 | 0.973 | 1.10 | 0.12 | 83.7 |
| 26 | 0.973 | 1.15 | 0.04 | 93.5 |
| 27 | 0.973 | 1.15 | 0.06 | 92.0 |
| 28 | 0.973 | 1.15 | 0.08 | 93.0 |
| 29 | 0.973 | 1.15 | 0.10 | 85.0 |
| 30 | 0.973 | 1.15 | 0.12 | 88.5 |
| 31 | 2.000 | 1.00 | 0.04 | 84.6 |
| 32 | 2.000 | 1.00 | 0.06 | 85.2 |
| 33 | 2.000 | 1.00 | 0.08 | 84.9 |
| 34 | 2.000 | 1.00 | 0.10 | 79.3 |
| 35 | 2.000 | 1.00 | 0.12 | 75.2 |
| 36 | 2.000 | 1.10 | 0.04 | 93.0 |
| 37 | 2.000 | 1.10 | 0.06 | 91.4 |
| 38 | 2.000 | 1.10 | 0.08 | 89.5 |
| 39 | 2.000 | 1.10 | 0.10 | 86.2 |
| 40 | 2.000 | 1.10 | 0.12 | 84.6 |

## Experimental and Calculated Results

For the purpose of comparing mathematical model predictions with experimental results, experiments with dodecylbenzene sulfonation were carried out at $SO_3$/DDB mole ratios of 1.00 and 1.10 for the three reactors; and in addition, for the 0.973 reactor, $SO_3$/DDB ratios of 1.05 and 1.15 were studied. For each reactor and mole ratio, five different $SO_3$ mole fractions in the gas, 0.04, 0.06, 0.08, 0.10, and 0.12, were established.

The $SO_3$ flow rate was fixed at $2.187 \times 10^{-3}$ mol/s for all experiments, and the DDB and $N_2$ flows were adjusted to obtained the desired $SO_3$/DDB mole ratio and $SO_3$ mole fraction in the gas for each experiment. So, the ranges of flow rates were $1.902 \times 10^{-3}$–$2.187 \times 10^{-3}$ mol of DDB/s and $1.604 \times 10^{-2}$–$5.249 \times 10^{-2}$ mol of $N_2$/s.

The sulfonated product was analyzed for active matter content by two-phase titration with Hyamine.

Every experiment was repeated to determine the experimental error, so that 80 experiments were carried out. Table III shows the experimental values for the mean active matter.

The mathematical model is considered valid if it is statistically significant at a 95% confidence level. The developed mathematical model has three parameters, $A_0$, $A_1$, and $B$, whose numberical values are unknown. They

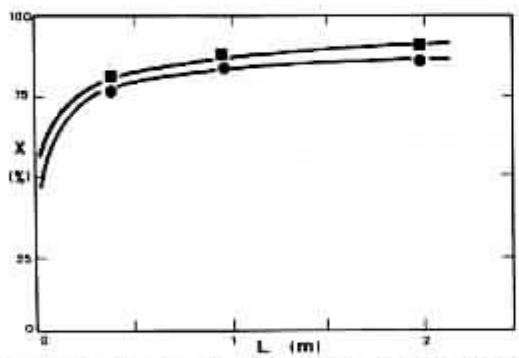


**Figure 8.** Conversion versus reactor length. Experimental points: (■) $SO_3$ mole fraction 0.08, $SO_3$/DDB mole ratio 1.10; (●) $SO_3$ mole fraction 0.08, $SO_3$/DDB mole ratio 1.00. Solid lines are the corresponding model predictions.

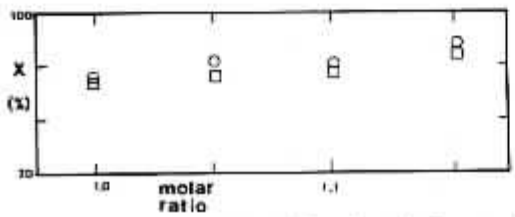


**Figure 9.** Conversion versus $SO_3$/DDB mole ratio. Reactor length: 1.00 m. $SO_3$ mole fraction: 0.06. (□) Model predictions. (○) Experimental points.

are determined from experimental results. A set of values for $A_0$, $A_1$, and $B$, which give a minimum for the function $\phi$, was searched:

$$\phi = \sum_{i=1}^{N} \left[ \frac{X_{mod} - X_{exp}}{X_{mod}} \right]^2$$

where $N$ is the number of experiments chosen for this fit. Six experiments including different values for the three studied variables, reactor length, $SO_3$/DDB mole ratio, and $SO_3$ mole fraction in the gas, were chosen for the fit. Their numbers were 3, 6, 10, 13, 21, and 25 (Table III).

The minimum for $\phi$ was found by the modified simplex method (Himmelblau, 1970).

The values obtained for the parameters were $A_0 = 14$, $A_1 = 0.060$, and $B = 0.30$.

The validity of the model was established by comparing its predictions with every experimental result. For every experiment, the model was solved with the parameter values previously determined and the corresponding values of the variables.

The comparison shows that the mathematical model is statistically significant at a 95% confidence level.

The variance of the fit is 3.2%, and the variance of the experimental error is 2.5%.

The concordance between model predictions and experimental results for examples of conversion variations with respect to the three studied variables can be graphically seen in Figures 8–10.

In Figure 8 experimental conversions and model predictions are plotted against reactor length for two different $SO_3$/DDB mole ratios. The model adequately predicts the variation in conversion experimentally obtained with reactor length; the greater part of conversion takes place at the beginning of the reactor, where the liquid mass-transfer resistance is smaller because of the great influence of the gas–liquid shear stress. Moreover, in this zone, liquid viscosity is smaller because of the small concentration of

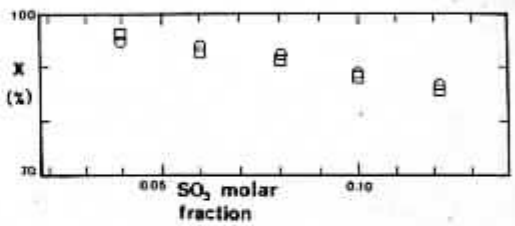


**Figure 10.** Conversion versus $SO_3$ mole fraction in the gas. Reactor length: 2.00 m. $SO_3$/DDB mole ratio: 1.10. (□) Model predictions. (○) Experimental points.

causes the variation in conversion to be much smaller in other zones of the reactor: the process rate is mainly controlled by liquid film mass transfer.

Models assuming that gas mass transfer is the only controlling step cannot predict this behavior. If these models are adjusted to predict such a high conversion for the reactor of 0.40-m length, they would predict practically total conversions for the 0.973- and 2.000-m lengths, especially for $SO_3$/DDB mole ratios greater than 1.

Considering liquid mass transfer, the high conversions obtained would not take place through a pure molecular mechanism because of the low diffusivities of such a viscous system, so it is necessary to consider turbulences in the system.

In Figure 9, variations of conversion versus $SO_3$/DDB mole ratios are shown. There are two factors that favor increase in conversion for increasing $SO_3$/DDB mole ratios: greater $SO_3$ concentrations in the gas, and lower DDB flow rate, and therefore smaller film thickness. However, the influence of $SO_3$/DDB mole ratio is not as important as it would be if gas mass transfer were the only controlling step. Liquid mass-transfer resistance restricts the increase in conversion. A good fit to experimental results is obtained when this resistance is included in the model.

In Figure 10, variations in conversion with $SO_3$ mole fraction in the gas are shown. It is clear from experimental results that conversion decreases when $SO_3$ mole fraction in the gas increases.

For the $SO_3$/DDB mole ratio constant, decreasing $SO_3$ mole fraction in the gas implies greater $N_2$ flow rate and therefore more turbulence in the gas. If gas-phase mass transfer is the only controlling step, this increase in turbulence would not balance the decrease of the driving force due to dilution. This model would not explain the variations in conversion that really takes place, and it would predict variations in opposite directions. It is necessary, therefore, to consider liquid-phase resistance.

When $SO_3$ mole fraction in the gas is decreased, the increase in gas flow rate causes a thinning of the film and a decrease in liquid-phase resistance to mass transfer. However, this thinning is not enough to explain the experimental increase in conversion. Our model takes into account the influence of the gas shear stress on the liquid mass-transfer resistance. This shear stress induces a greater turbulence in the liquid phase, decreasing its resistance to mass transfer. This fact explains the experimental behavior as it can be observed from the agreement between model predictions and experimental results represented in Figure 10.

The concordance obtained for this process indicates that the model could be applied to any process that takes place in a falling film reactor, since the sulfonation process described in this work is one of the more complicated cases that can be presented. Other possible processes—evaporation, refrigeration, etc.—would permit the as-

## Nomenclature

$A$ = parameter defined in eq 4
$A_\phi$ = parameter defined in eq 4
$A_i$ = parameter defined in eq 4
$B$ = parameter defined in eq 5
$C$ = concentration, kmol/m$^3$
$C_p$ = heat capacity, J/(kmol·K)
$D$ = diffusivity, m$^2$/s
$D_E$ = eddy diffusivity, m$^2$/s
$d$ = reactor diameter, m
$f$ = friction coefficient, dimensionless
$g$ = acceleration of gravity, m/s$^2$
$\Delta H_R$ = reaction enthalpy, J/kmol
$h_G$ = gas-to-liquid heat-transfer coefficient, J/(m$^2$·s·K)
$h_w$ = wall to refrigerated water heat-transfer coefficient, J/(m$^2$·s·K)
$K_L$ = liquid thermal conductivity, J/(m·s·K)
$K_w$ = wall thermal conductivity, J/(m·s·K)
$K_G$ = gas-phase mass-transfer coefficient, m/s
$k$ = reaction rate constant, m$^3$/(kmol·s)
$L$ = reactor length, m
$m$ = $SO_3$ Henry's constant, (kmol of $SO_3$/m$^3$ of gas)/(kmol of $SO_3$/m$^3$ of liquid)
$N$ = absorption rate per unit of area, kmol/(m$^2$·s)
$r$ = reaction rate, kmol/(m$^3$·s)
$T$ = temperature, K
$U$ = gas mean velocity, m/s
$U_L$ = global heat-transfer coefficient, J/(m$^2$·s·K)
$u$ = gas velocity, m/s
$u_0$ = turbulence characteristic velocity of gas, m/s
$V$ = liquid mean velocity, m/s
$v$ = liquid velocity, m/s
$X$ = conversion, dimensionless
$y$ = transversal coordinate, m
$y^+$ = dimensionless transversal coordinate, $yu_0/\nu$
$z$ = axial coordinate, m

### Greek Symbols

$\alpha$ = thermal diffusivity, m$^2$/s
$\alpha_E$ = eddy thermal diffusivity, m$^2$/s
$\Gamma$ = flow per perimeter unit, m$^2$/s
$\phi$ = dimensionless function defined in eq 19
$\delta$ = film thickness, m
$\delta^+$ = dimensionless film thickness, $\delta u_0/\nu$
$\mu$ = dynamic viscosity, kg/(m·s)
$\nu$ = kinematic viscosity, m$^2$/s
$\rho$ = density, kg/m$^3$
$\tau$ = interfacial shear stress, Pa

### Subscripts and Superscripts

E = eddy
ex = exterior
G = in gas phase
i = in the interface
in = interior
L = in liquid phase
lm = logarithmic mean
R = of the refrigerated water
w = in the wall

**Registry No.** Dodecylbenzene, 123-01-3.

## Literature Cited


Bird, R. B.; Steward, W. E.; Lightfoot, E. N. *Transport Phenomena*; Wiley: New York, 1960.
Brönstrom, A. *Trans. Inst. Chem. Eng.* **1975**, *53*, 29.
Cook, R. A.; Reginald, H. C. *Ind. Eng. Chem. Fundam.* **1973**, *12*, 106.
Davies, J. T. *Turbulence Phenomena*; Academic: New York, 1972.
Davis, E. J.; David, M. M. *Ind. Eng. Chem. Fundam.* **1964**, *3*, 111.
Davis, E. J.; Ouwerkerk, M. V.; Venkatesh, S. *Chem. Eng. Sci.* **1979**, *34*, 539.
Gilliland, E. R.; Sherwood, T. K. *Ind. Eng. Chem.* **1934**, *26*, 516.
Henstock, V. H.; Hanratty, T. J. *AIChE J.* **1979**, *25*, 122.
Himmelblau, D. M. *Process Analysis by Statistical Methods*; Wiley: New York, 1970.
Jepsen, J. C.; Crosser, O. K.; Perry, R. H. *AIChE J.* **1966**, *12*, 186.
Johnson, G. R.; Crynes, B. L. *Ind. Eng. Chem. Process Des. Dev.* **1974**, *13*, 6.
Lapidus, L. *Digital Computation for Chemical Engineers*; McGraw-Hill: New York, 1962.
Levich, V. G. *Physicochemical Hydrodynamics*; Prentice-Hall: Englewood Cliffs, NJ, 1962.
Mann, R.; Moyes, H. *AIChE J.* **1977**, *23*, 17.
Mann, R.; Knish, P.; Allan, J. C. *ACS Symp. Ser.* **1982**, *196*, 1.
McReady, M. J.; Hanratty, T. J. In *Gas Transfer at Water Surfaces*; D. Reidel: Dordrecht, Holland, 1984.
Pierson, F. W.; Whitaker, S. *Ind. Eng. Chem. Fundam.* **1977**, *16*, 401.
Reid, R. C.; Prausnitz, J. M.; Sherwood, T. K. *The Properties of Gases and Liquids*; McGraw-Hill: New York, 1977.
Yih, S.; Liu, J. *AIChE J.* **1983**, *29*, 903.


*Received for review* April 9, 1987
*Revised manuscript received* January 6, 1988
*Accepted* February 8, 1988

# Modeling of Thermal Oxidation of Silicon